Covalent-Ionically Crosslinked Sulfonated Poly(arylene ether sulfone)s Bearing Quinoxaline Crosslinkages As Proton Exchange Membranes

Pei Chen,[1,2] Xinbing Chen,[1,2] Zhongwei An[1,3]

[1]*Key Laboratory of Applied Surface and Colloid Chemistry of Ministry of Education, Shaanxi Normal University, Xi'an 710062, People's Republic of China*
[2]*School of Materials Science and Engineering, Shaanxi Normal University, Xi'an 710062, People's Republic of China*
[3]*Xian Modern Chemistry Research Institute, Xi'an 710065, People's Republic of China*

Received 17 May 2011; accepted 18 November 2011
DOI 10.1002/app.36517
Published online 22 January 2012 in Wiley Online Library (wileyonlinelibrary.com).

ABSTRACT: Crosslinkable sulfonated poly(arylene ether sulfone)s (SPAESs) were synthesized by copolymerization of 4,4′-biphenol with 2,6-difluorobenzil, 4,4′-difluorodiphenyl sulfone, and 3,3′-disulfonated-4,4′-difluorodiphenyl sulfone disodium salt. The corresponding covalent-ionically crosslinked SPAESs were prepared via the cyclocondensation reaction of benzil moieties in polymer chain with 3,3′-diaminobenzidine. The crosslinking significantly improved the membrane performance, that is, the crosslinked membranes had the lower membrane dimensional swelling, lower methanol permeability, and higher oxidative stability than the corresponding precursor membranes, with keeping the reasonably high proton conductivity. The crosslinked membrane (**CS5**) with measured ion exchange capacity of 1.47 meq g^{-1} showed a reasonably high proton conductivity of 112 mS cm^{-1} with water uptake of 42 wt % at 80°C, and exhibited a low methanol permeability of 2.1×10^{-7} cm^2 s^{-1} for 32 wt % methanol solution at 25°C. The crosslinked SPAES membranes have potential for PEFC and DMFCs. © 2012 Wiley Periodicals, Inc. J Appl Polym Sci 124: E278–E289, 2012

Key words: crosslinked sulfonated poly(arylene ether sulfone); proton exchange membrane; quinoxaline groups; methanol permeability

INTRODUCTION

In the past decades, as one of the most promising clean energy sources for transportation, stationary and portable power applications, polymer electrolyte membrane (PEM) fuel cells (PEFCs), and direct methanol fuel cells (DMFCs) have attracted considerable attentions due to their high efficiency and low pollution to environment.[1,2] PEM is one of the key components in PEFC and DMFC systems, and serves as a proton conductor and a fuel separator between anode and cathode. Perfluorosulfonate polymer membranes such as DuPont's Nafion membranes are the state-of-art PEMs commercially available with features of high proton conductivity and excellent chemical stability.[3] However, large fuel crossover, lower operating temperature below 80°C, and high cost critically limit their widespread application.[4] Therefore, sulfonated aromatic polymers have been extensively studied as alternative PEMs.[4–25]

Despite extensive efforts, however, the performance of alternative PEMs is still inferior to that of perfluorosulfonate polymer membranes. Consequently, further improvement of alternative materials is essential. Among alternative PEM materials, sulfonated poly(arylene ether)s (SPAEs) such as sulfonated poly(arylene ether sulfone)s (SPAESs)[13–19] and sulfonated poly(arylene ether ketone)s (SPAEKs)[20–22] are widely considered as one of the promising candidates for fuel cell applications due to their good thermal and chemical stability and good proton conductivity. Various factors such as levels of sulfonation (or ion exchange capacity, IEC), the solvents used for casting the membranes, and the membrane preconditioning are found to affect the properties such as the water uptake (WU), the membrane swelling, and the proton conductivity of SPAEs, and membrane electrode assembly performance due to variations in the microstructure. It is known that most of SPAEs with high

Correspondence to: X. Chen (chenxinbing@snnu.edu.cn).
Contract grant sponsor: Key Technologies R&D Program of Shaanxi Province; contract grant number: 2009K06-08.
Contract grant sponsor: Program for Changjiang Scholars and Innovative Research Team in University; contract grant number: IRT1070.
Contract grant sponsor: Fundamental Research Funds for the Central Universities; contract grant numbers: GK200902002, GK201002002.
Contract grant sponsors: Scientific Research Foundation for Returned Scholars, Ministry of Education, the Youth Foundation of School of Chemistry and Materials Science, Shaanxi Normal University.

IEC makes them excessively swell and even soluble in water, resulting in a lower membrane stability. To overcome this problem, several methods have been developed, such as covalently crosslinked membranes,[26–32] ionically crosslinked acid/base blend membranes[33–35] and layer-by-layer membranes,[36–39] in which the formation of strong and stable crosslinking bonds is a common and powerful method to suppress membrane swelling and to improve the membrane durability. However, some of the covalent crosslinking methods are achieved via the crosslinking mechanism involving elimination of sulfuric acid groups, which results in a decrease in ion content of the membrane. To avoid the consumption of sulfuric acid in polymer, unsaturated propenyl-based crosslinkable SPAEs have been developed.[30–32] The corresponding crosslinked SPAEs obtained via thermally crosslinking method exhibit improved properties.

Recently, an improved crosslinking strategy based on elimination of sulfuric acid in SPAEs is developed via the formation of sulfonamide linkage, where sulfonated diamine-based crosslinking agent helps to compensate the loss of sulfuric acid groups in polymer.[40] In our recent research, both covalent crosslinking and ionic acid-base crosslinking could be achieved by introducing quinoxaline crosslinkages in the SPAEK membranes, and the resulting membranes displayed the improved properties compared with the uncrosslinked ones.[41] However, in order to clearly investigate the effects of the crosslinking on the membrane properties, the IECs of the studied SPAEK membranes were limited to be higher than 2.0 meq g^{-1}, which made the crosslinked SPAEK membrane swell strongly at 80°C. Meanwhile, a side-chain type of activated difluoro monomer, 2,6-difluorobenzil (DFB), used as the nonsulfonated monomer and crosslinkable group, was not helpful for increasing the mechanical property of the SPAEK membranes due to the rigid structure of the formed nonsulfonated parts. Generally, a flexible and activated main-chain difluoro monomer should be helpful. In this work, we present crosslinkable SPAESs composed of benzil moieties and flexible sulfonated and nonsulfonated monomers, and prepare a series of quinoxaline-based crosslinked SPAESs with IECs less than 2.0 meq g^{-1} via the cyclocondensation reaction of benzil moieties in polymer chain with 3,3′-diaminobenzidine (DAB) to form quinoxaline groups, which act as covalent and acid-base ionic crosslinking. For the crosslinked membranes with different quinoxaline capacity (QC), the properties including WU, membrane swelling, proton conductivity, mechanical property, oxidative stability, and methanol permeability are investigated, compared with the corresponding precursor membranes.

EXPERIMENTAL

Materials

4,4′-Biphenol (BP) and DAB were purchased from Aladdin-reagent Co. (Shanghai, China) and BP was purified by vacuum sublimation prior to use. 4,4′-Difluorodiphenyl sulfone (DFDPS) were purchased from Zhejiang Shouerfu Chemical Co. (Lishui, China) and purified by vacuum sublimation prior to use. Dimethyl sulfoxide (DMSO), *N*,*N*-dimethylacetamide (DMAc), *N*,*N*-dimethylformamide (DMF), and 1-methyl-2-pyrrolidone (NMP) were purchased from Sinopharm Chemical Reagent Co. (Shanghai, China) and dehydrated with molecular sieve 4A. Fuming sulfuric acid (20% SO_3), calcium hydride, and other materials were purchased from Sinopharm Chemical Reagent Co. (Shanghai, China) and used as received. NMP was dehydrated by calcium hydride, distilled under reduced pressure, and then dried with molecular sieve 4A prior to use. 3,3′-Disulfonated-4,4′-difluorodiphenyl sulfone disodium salt (SDFDPS) was prepared by sulfonation of DFDPS at 120°C using fuming sulfuric acid. DFB was prepared according to the literature.[41]

Polymerization

SPAES copolymer BP-SDFDPS/DFDPS/DFB(x/y/z), where the data in parenthesis refer to the molar ratio of SDFDPS : DFDPS : DFB, was prepared by a one-pot high temperature polymerization method, as shown in Scheme 1. As an example, the preparation procedure of BP-SDFDPS/DFDPS/DFB(1/0.5/0.5), **S1** in Table I, is described below.

To a 100-mL dry three-neck flask equipped with a Dean-Stark trap and a condenser, 2.292 g (5.0 mmol) of SDFDPS, 0.636 g (2.5 mmol) of DFDPS, 0.616 g (2.5 mmol) of DFB, 1.862 g (10.0 mmol) of BP, 1.588 g (11.5 mmol) of anhydrous potassium carbonate, 26 mL of NMP, and 15 mL of toluene were added under nitrogen flow with stirring. The reaction mixture was heated to 140°C. Water and toluene were evaporated as the azeotrope and collected in the Dean–Stark trap. After water was completely evaporated (the Dean–Stark trap became clear), the reaction temperature was raised to 160°C and the polymerization was continued at this temperature for 10 h. The resulting highly viscous solution was slowly poured into water. The resulting fiber-like precipitate was thoroughly washed in water with stirring at 50°C overnight, and then washed with methanol, and dried at 120°C in vacuum.

Crosslinked SPAES copolymer, BP-SDFDPS/DFDPS/DFB/DAB(x/y/z/w), where the data in parenthesis (x/y/z/w) refer to the molar ratio of SDFDPS : DFDPS : DFB : DAB, was prepared by using the cyclocondensation reaction of benzil groups in DFB moieties and DAB to form quinoxaline, as shown in Scheme 1. Here, the molar content

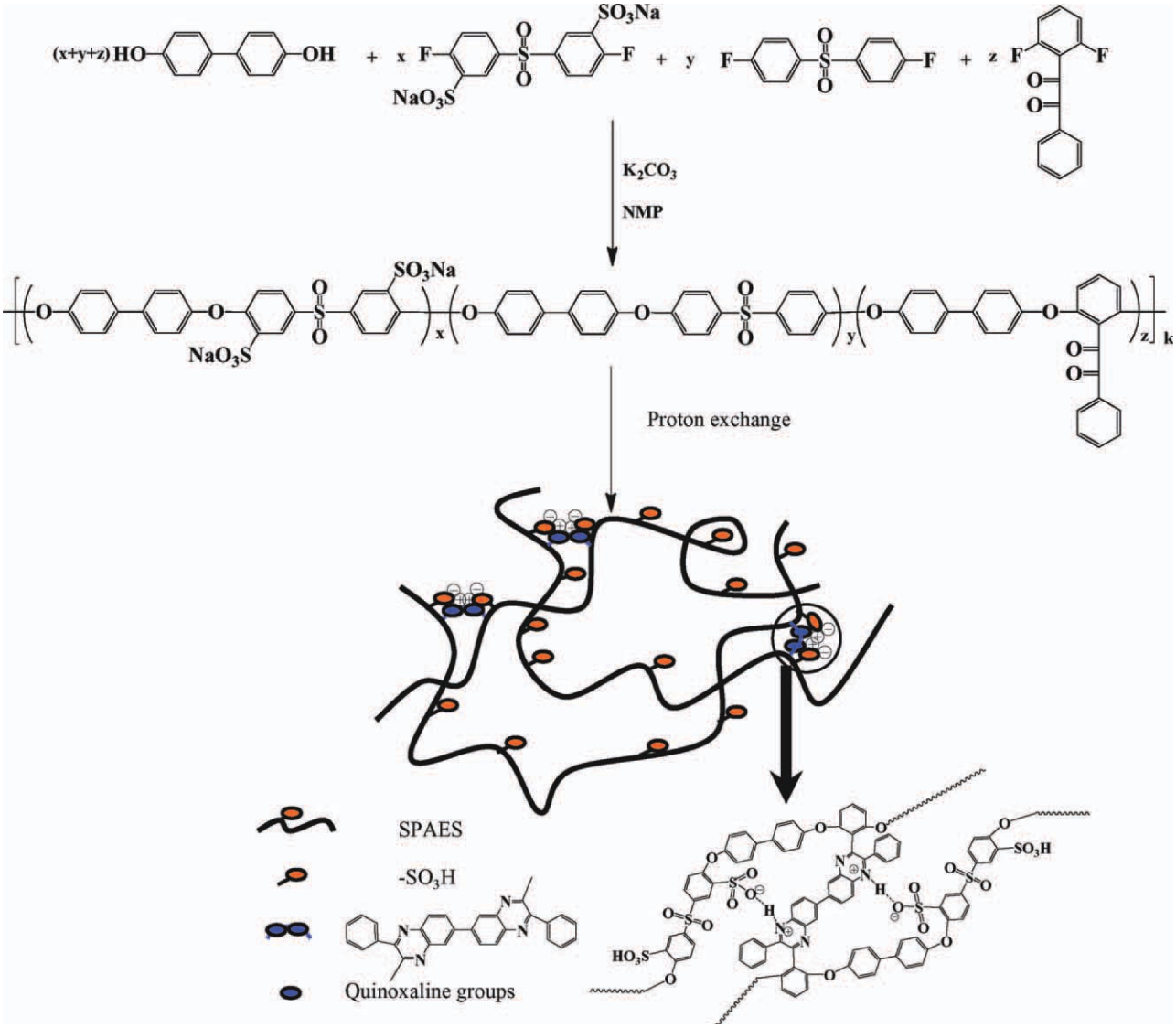

Scheme 1 Preparation of crosslinkable SPAESs and corresponding crosslinked membranes. [Color figure can be viewed in the online issue, which is available at wileyonlinelibrary.com]

of DAB was set as 30 mol % based on DFB for all the crosslinked membranes, that is, $w = 0.3z$. As an example, the crosslinked polymer of BP-SDFDPS/DFDPS/DFB/DAB(1/0.5/0.5/0.15), **CS1** in Table I, is described below.

A 7 wt % BP-SDFDPS/DFDPS/DFB(1/0.5/0.5) solution in DMSO was prepared and filtrated. A given amount of DAB was added into the filtrate and the mixture was stirred at 140°C for 4 h and then 160°C for 4–5 h (the gelation took place if the reaction was continued for a longer time) under nitrogen protection. Then, the crosslinked polymer solution was obtained and cooled to 80°C for the following membrane casting.

In our experiment, the solution was directly casted onto glass plates to prepare the crosslinked membrane without separation and process of the crosslinked polymer.

Membrane formation and proton exchange

Uncrosslinked SPAES membrane

A 7 wt % SPAES solution in DMSO was prepared and filtrated. The filtrate was cast onto glass plates at 80°C, and dried at 100°C for 12 h. The as-cast membranes were soaked in water at 40°C for 48 h, and proton-exchanged with 1*M* hydrochloric acid at 50°C for 48 h. The proton-exchanged membranes were thoroughly washed with deionized water till the rinsed water became neutral, followed by drying in vacuum at 120°C for 15 h. The membranes obtained were 40–60 μm in thickness.

Crosslinked SPAES membrane

The 7 wt % crosslinked polymer solution obtained as aforementioned was cooled and cast onto glass

TABLE I
Basic Properties of SPAES Membranes[a]

Code	Membranes	IEC[b] (meq g^{-1})	QC (meq g^{-1})	MU[c] (%)	SU[c] (%)	WU (%) 25°C	WU (%) 80°C	λ[d] 25°C	λ[d] 80°C	Size change[e] Δt_c	Size change[e] Δl_c	$\Delta_{t/l}$[e]
S1	BP-SDFDPS/DFDPS/DFB(1/0.5/0.5)	2.00 (1.97)	–	D	215	56	139	16	39	0.34	0.32	1.06
CS1	BP-SDFDPS/DFDPS/DFB/DAB(1/0.5/0.5/0.15)	1.96 (1.78)	0.30	118	111	43	81	13	25	0.22	0.21	1.05
S2	BP-SDFDPS/DFDPS/DFB(1/0.5/0.7)	1.85 (1.84)	–	359	181	48	105	14	32	0.27	0.27	1.00
CS2	BP-SDFDPS/DFDPS/DFB/DAB(1/0.5/0.7/0.21)	1.80 (1.55)	0.39	53	59	30	54	11	19	0.14	0.15	0.93
S3	BP-SDFDPS/DFDPS/DFB(1/0.7/0.5)	1.85 (1.84)	–	397	170	47	108	14	33	0.28	0.27	1.04
CS3	BP-SDFDPS/DFDPS/DFB/DAB(1/0.7/0.5/0.15)	1.81 (1.62)	0.28	53	76	34	59	12	20	0.16	0.16	1.00
S4	BP-SDFDPS/DFDPS/DFB(1/0.7/0.8)	1.67 (1.63)	–	60	60	37	60	13	20	0.16	0.17	0.94
CS4	BP-SDFDPS/DFDPS/DFB/DAB (1/0.7/0.8/0.24)	1.62 (1.34)	0.40	37	36	26	37	11	15	0.11	0.11	1.00
S5	BP-SDFDPS/DFDPS/DFB(1/1/0.5)	1.66 (1.65)	–	57	66	40	65	12	22	0.18	0.17	1.06
CS5	BP-SDFDPS/DFDPS/DFB/DAB (1/1/0.5/0.15)	1.64 (1.47)	0.25	39	47	29	42	11	16	0.12	0.12	1.00
CS2–2	BP-SDFDPS/DFDPS/DFB/DAB(1/0.5/0.7/0.30)	1.78 (1.37)	0.53	37	41	27	39	11	16	0.11	0.11	1.00
CS4–2	BP-SDFDPS/DFDPS/DFB/DAB (1/0.7/0.8/0.32)	1.61 (1.23)	0.51	30	31	22	31	10	14	0.091	0.094	0.97
R1	BP-SDFDPS/DFDPS(1/1)	1.99 (1.97)	–	D	110	90	184	25	51	0.40	0.41	0.98
R2	BP-SDFDPS/DFB(1/1)	2.01 (1.96)	–	S + D	70	62	99	17	27	0.31	0.29	1.07

[a] The experimental errors for IEC, MU, SU, WU, and size change were ±1, ±2, ±2, ±2, and ±3%, respectively.
[b] Calculated value; the data in parentheses are obtained by a titration method.
[c] At 25°C; S and D represent swollen and dissolved, respectively.
[d] Based on measured IEC, $\lambda = WU \times 10/(18 \times IEC)$.
[e] At 80°C.

plates at 80°C, and dried at 100°C for 4 h, 120°C for 2 h, and then cured at 180°C in vacuum for 5 h *to promote the crosslinking reaction*. The as-cast membranes were post-treated as mentioned above.

Characterization and measurements

FT-IR spectra were recorded on a Bruker Equinox 55 spectrometer. NMR spectra were recorded on a Bruker AV 300 (300 MHz) instrument. Thermogravimetric analysis (TGA) was carried out with a TA 600SDT in helium (flow rate: 100 cm^3 min^{-1}) at a heating rate of 10°C min^{-1}, standing at 150°C for 0.5 h. Mechanical tensile tests were performed on a universal testing machine (CTM6001) at 25°C and about 30% relative humidity at a crosshead speed of 5 mm min^{-1}. Solubility tests were carried out in DMAc, DMF, NMP, and DMSO with a concentration of 5% (w/v) at room temperature. The reduced viscosity (η_r) was measured with an Ubbelohde viscometer using 0.5 g dL^{-1} DMSO solution of SPAES in sodium salt form at 35°C. Molecular weight measurement was performed via gel permeation chromatography (GPC) with Waters-Breeze 1515. DMF was used as the eluant (0.1% LiCl was added to inhibit aggregation) and the μ-Styragel column was calibrated by polystyrene standards.

IEC was calculated from the molar ratio of sulfonated difluoride monomer to nonsulfonated one in feed, and also evaluated by a titration method. A sample membrane in proton form was soaked in a 15 wt % NaCl solution at 40°C for 72 h and the released proton was titrated with a 0.05*M* NaOH solution, using phenolphthalein as an indicator. The titration was carried out for the solutions containing the sample membranes within a few minutes.

QC defined as the molar amount of quinoxaline groups per unit weight (meq g^{-1}) was calculated from the molar ratio of crosslinking reagent DAB to nonsulfonated difluoride monomer DFB in feed.

WU of membrane was obtained by calculating the weight difference between the dry and wet membranes. The completely dried membrane samples were weighed and then soaked into deionized water until the weight remained constant. Then the samples were taken out, wiped with tissue paper, and quickly weighted on a microbalance. The WU was calculated, using the following equation:

$$\mathrm{WU} = [(W_s - W_d)/W_d] \times 100\% \quad (1)$$

where W_s and W_d are the weights of swollen and dry membranes, respectively.

Methanol uptake (MU) and solvent uptake (SU) were measured by the following procedure: sample membranes were dried at 120°C under vacuum for 8 h to get the dry weight (W_d). Then, the sample membranes were immersed in methanol or 50% methanol solution in a sealed bottle at 25°C until the weight remained constant, and then taken out, wiped with tissue paper, and quickly weighted on a microbalance to get the wet weight (W_m or W_{mw} for methanol or 50% methanol solution, respectively). The MU and SU were calculated from eq. (2):

$$\begin{aligned} \mathrm{MU} &= [(W_m - W_d)/W_d] \times 100\% \\ \mathrm{SU} &= [(W_{\mathrm{mw}} - W_d)/W_d] \times 100\% \end{aligned} \quad (2)$$

Dimensional change of membrane was measured by soaking more than two sample sheets in water at different temperatures. The *through-plane* and *in-plane* dimensional changes (Δt_c and Δl_c) and the membrane swelling ratio ($\Delta_{t/l}$) were calculated from eq. (3):

$$\begin{aligned} \Delta t_c &= [(t - t_d)/t_d] \times 100\% \\ \Delta l_c &= [(l - l_d)/l_d] \times 100\% \\ \Delta_{t/l} &= \Delta t_c/\Delta l_c \end{aligned} \quad (3)$$

where t_d and l_d are the thickness and length of the dry membrane, respectively; t and l refer to those of the membrane immersed in water.

Proton conductivity of membrane was determined using an electrochemical impedance spectroscopy technique over the frequency from 100 Hz to 100 kHz (Hioki 3532-80). A single cell with two platinum plate electrodes was mounted on a Teflon plate at 0.5-cm distance. A membrane swollen in water at 25°C was set in the cell. The cell was placed in deionized water. Proton conductivity was calculated from eq. (4):

$$\sigma = d/(t_s w_s R) \quad (4)$$

where d is the distance (or membrane length) between the two electrodes, t_s and w_s are the thickness and width of the membrane in deionized water, respectively, and R is the measured resistance value. The d, t_s, and w_s values at different temperatures were evaluated from the temperature dependence of dimensional change of membrane.

Oxidative stability was determined using Fenton's reagent (3 wt % H_2O_2 + 2 ppm $FeSO_4$) at 80°C. The membranes (50–60 μm in thickness) were immersed in Erlenmeyer flasks containing Fenton's reagent. The flasks were shaken vigorously once every 10 min until the membranes begin to break.

Methanol permeability (P_M) measurement was carried out using a liquid permeation cell composed of two compartments, which were separated by a vertical membrane. The membrane was first immersed in water for 2 h to get the water-swollen sample and then set into the measurement cell (effective area: 16 cm^2). One compartment of the cell (V_a = 400 mL) was filled with 32 wt % methanol feed solution, and the other compartment (V_b = 90 mL) was filled with deionized water. The compartments were stirred continuously during the permeability measurement. The methanol concentrations of the two compartments were analyzed with a Shimadzu GC2014C gas chromatography apparatus. Methanol permeability, P_M, was calculated from eq. (5):

$$P_M = kV_bL/(AC_a) \quad (5)$$

where k is the slope of the straight-line plot of methanol concentration in permeate versus permeation time, C_a refers to the methanol concentration in feed, V_b is the solution volume of the permeate. L and A refer to the thickness and effective area of the swollen membrane, respectively.

RESULTS AND DISCUSSION

Characterization of crosslinkable SPAES

Table I lists crosslinkable SPAES copolymers prepared in this study (**S1**–**S5**) and their fundamental properties. The molar ratio of sulfonated monomer to nonsulfonated one was set in the range of 1/1-1/1.5 to ensure the copolymers with calculated IECs of 1.66–2.00 meq g^{-1}. The IEC values determined by the titration method were as large as 98% of the corresponding theoretical values, which indicates that the proton exchange was almost complete for SPAESs. The polymerization results and molecular weights are listed in Table II. The copolymers were prepared with high yields of 90–95% and had high reduced viscosities ranged from 1.0 to 1.2 dL g^{-1}, which was in accordance with their high molecular weights. Molecular weight distributions ($\overline{M}_w/\overline{M}_n$), measured by GPC in DMF, were in the range of 1.5–1.6, indicating a typical polycondensation procedure.

The chemical structure was identified by NMR and IR spectra. Figure 1(a) shows the ^{1}H NMR spectra of **S2** and **S4**. The signals at 8.3 and 7.96 ppm were assigned to the aromatic hydrogen atoms H9 and H8 at the *ortho* and *para* positions to the electron-withdrawing —SO_3H group, respectively, indicating incorporation of sulfonated difluoro monomer SDFDPS into polymer. Comparing the ^{1}H NMR spectra of the copolymers with that of DFDPS, the peak at 7.93 ppm was assigned to the proton H17 that lied on the *ortho* position to the sulfone group

TABLE II
Polymerization Results and Molecular Weight

Code	Yield (%)	H9/H5[a]		η_r[b] (dL g^{-1})	$\overline{M}_n$[c] (g mol^{-1})	$\overline{M}_w$[c] (g mol^{-1})	$\overline{M}_w/\overline{M}_n$
		Theoretical	^{1}H NMR				
S1	95	0.50	0.50	1.2	194,428	298,577	1.5
S2	90	0.70	0.71	1.0	198,042	306,361	1.5
S3	93	0.50	0.51	1.1	185,044	288,241	1.6
S4	91	0.80	0.79	1.0	198,435	301,073	1.5
S5	93	0.50	0.49	1.1	202,425	320,976	1.6
R2	94	1.00	1.01	1.2	192,041	296,258	1.5

[a] The mole ratio of nonsulfonated monomer DFB to sulfonated monomer SDFDPS.
[b] Reduced viscosity measured at 0.5 g dL^{-1} in DMSO in sodium salt form at 35°C.
[c] Determined by GPC in DMF (0.1% LiCl).

of DFDPS, where the peaks of H17 and H8 were close to each other because H17 was located in a similar local chemical environment to H8. The proton peak at 6.84 ppm was assigned to the aromatic hydrogen atom H24 at the *ortho* position to ether bonding in polymer main chain and at *meta* position to 1,2-dione group of DFB, according to the spectra of DFB and DFB-based polymer, R2 in Table I. The other overlapped peaks were also assigned according to the spectra of SDFDPS, DFDPS, DFB, and BP, as shown in Figure 1(a). Figure 1(b) shows the ^{13}C NMR spectrum of **S2**. Carbon atoms linked to oxygen or sulfur atoms (C═O, C─O, C─S) were discerned by their well-known and expected chemical shifts, where the peaks at 190.7, 191.2, and 139.4 ppm were assigned to the C═O carbon atoms and the carbon atom linked to the ─SO_3H group, respectively. Other carbon signals were assigned by using one bond ^{1}H-^{13}C correlation, as shown in Figure 1. The above data provided the evidence that three difluoro monomers, SDFDPS, DFDPS, and DFB, were incorporated in the obtained SPAESs.

Integration of ^{1}H NMR signals was used to calculate the sulfonation content that represents the actual mole percentage of sulfonated unit per average repeat unit in the obtained copolymers. As shown in Figure 1(a), only two characteristic peaks with single signal each other, proton H9 in SDFDPS and proton H24 in DFB, were possible to obtain accurate integration values. Then, the integrated intensity ratio of DFB proton H24 to SDFDPS proton H9 (H24/H9) was used for the calculation, as shown in Table II. The ratios of H24/H9 were found to be 0.50, 0.71, 0.51, 0.79, and 0.49 for **S1**, **S2**, **S3**, **S4**, and **S5**, respectively, which agreed with the theoretical ratios (0.50, 0.70, 0.50, 0.80, and 0.50, respectively). The results showed that the sulfonation content determined by the ^{1}H NMR method was in good agreement with the one calculated from the feed molar ratio within the difference of ±2 mol %, which implied that the polymerization was performed completely.

Figure 2 shows the IR spectrum of **S2**. The absorption bands at 1660 and 1740 cm^{-1} were assigned to symmetric and asymmetric stretching vibrations of C═O. The symmetric and asymmetric vibration of O═S═O bond of sulfonic acid group and sulfone group appeared at 1029, 1089, and 1166 cm^{-1}. The 1242 cm^{-1} peak was attributed to the vibrations of C─O─C group in aryl ether backbone.

Crosslinked SPAES

Table I also lists crosslinked SPAES membranes (**CS1**–**CS5**) and their fundamental properties. The formation of crosslinking was confirmed by IR measurement and also judged by the reduced solubility of the crosslinked membranes in common aprotic solvents in which the corresponding uncrosslinked membranes were well soluble. Figure 2 shows the IR spectra of the uncrosslinked and crosslinked membranes (**S2** and **CS2**, respectively). Although the two spectra were similar, the following differences were observed for **CS2**. The strong peak appeared at 1203 cm^{-1} was assigned to the characteristic stretching vibration of C─N. Although overlapping with that of phenyl ring (1471 cm^{-1}), the characteristic absorption bands of quinoxaline ring resulted in a strong shoulder peak at 1493 cm^{-1}. In addition, compared to **S2**, the shoulder peak at 1680 cm^{-1} for **CS2** was attributed to the vibration of C═N of quinoxaline ring. These indicated the formation of quinoxaline ring. The characteristic absorption bands of amino group at 3000–3400 cm^{-1} was not detected for **CS2** in sodium salt form as well as in proton form, indicating the absence of the unreacted diamino-phenyl end-groups. It was confirmed that the crosslinking of SPAES was performed well with the formation of the quinoxaline crosslinkage.

As listed in Table I, the IEC values determined by titration method were very close to the calculated IEC values for the uncrosslinked SPAES membranes (**S1-S5**, **R1**, and **R2**), whereas they were 9–17% smaller than the calculated ones for the crosslinked membranes (**CS1**–**CS5**). This was due to the formation of acid-base complex between sulfonic acid groups and quinoxaline moieties. For example, **CS2**, with

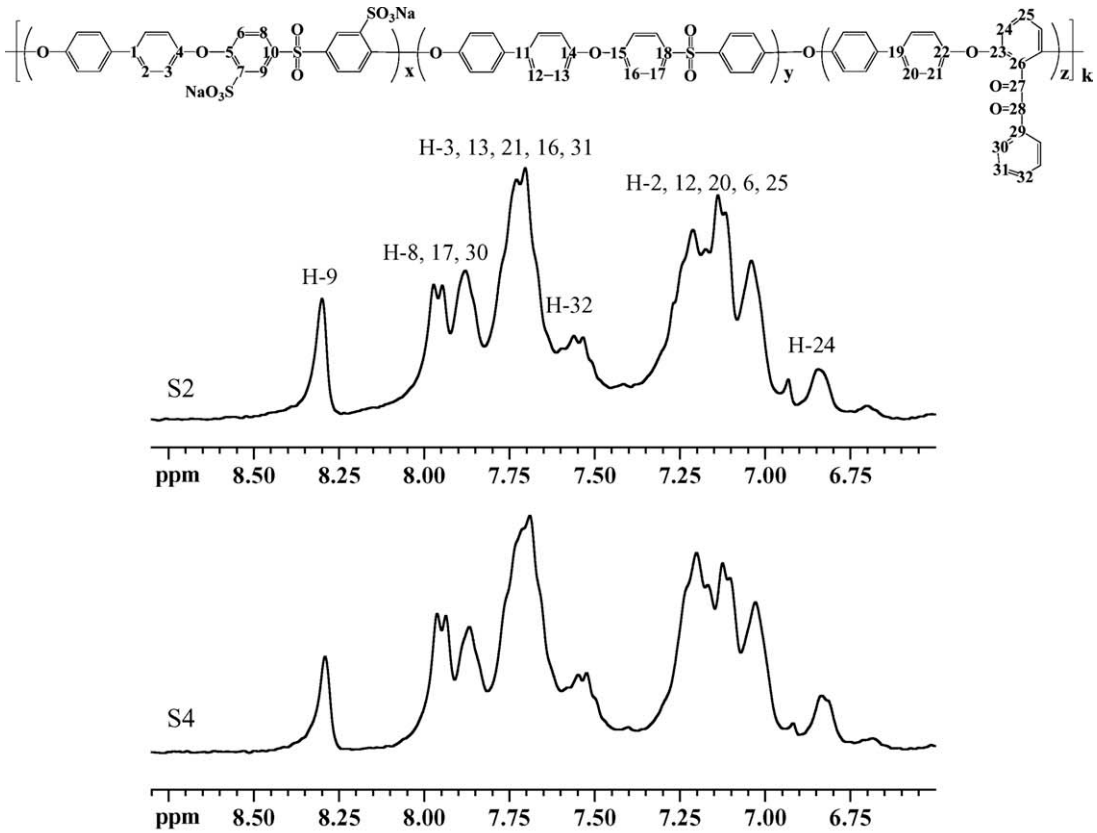

(a) ^{1}H NMR spectra of **S2** and **S4**

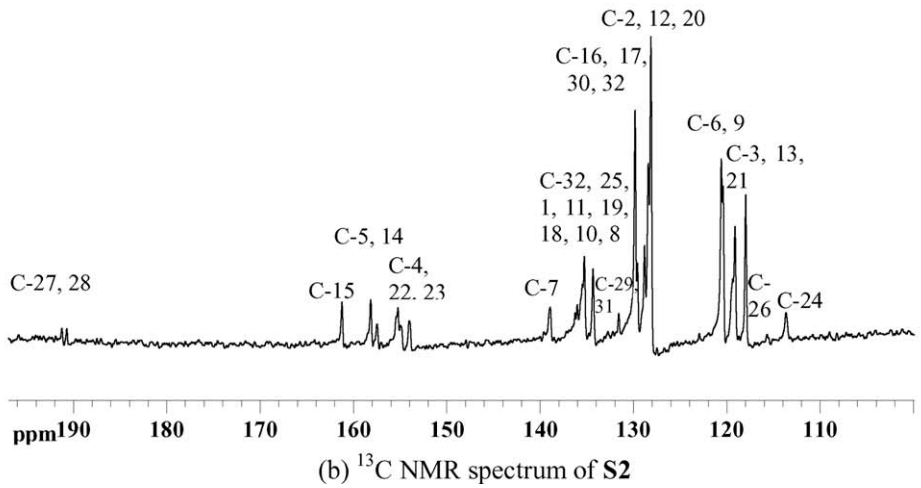

(b) ^{13}C NMR spectrum of **S2**

Figure 1 NMR spectra of SPAES membranes in proton form in DMSO-d_6.

calculated IEC of 1.80 meq g^{-1} and QC of 0.39 meq g^{-1}, exhibited a titrated IEC value of 1.55 meq g^{-1}. If sulfonic acid groups form the acid-base complex with all the quinoxaline groups to become unexchangeable with Na^{+} ions, the titrated IEC value will be close to the value subtracted QC from the calculated IEC. In the case of **CS2**, this value was 1.41 meq g^{-1}, which was slightly smaller than the titrated IEC value. Therefore, the titrated IEC value is considered as the effective IEC value.

Solubility, mechanical properties, thermal and oxidative stability

The solubility properties of SPAESs are listed in Table III. The uncrosslinked SPAESs generally showed

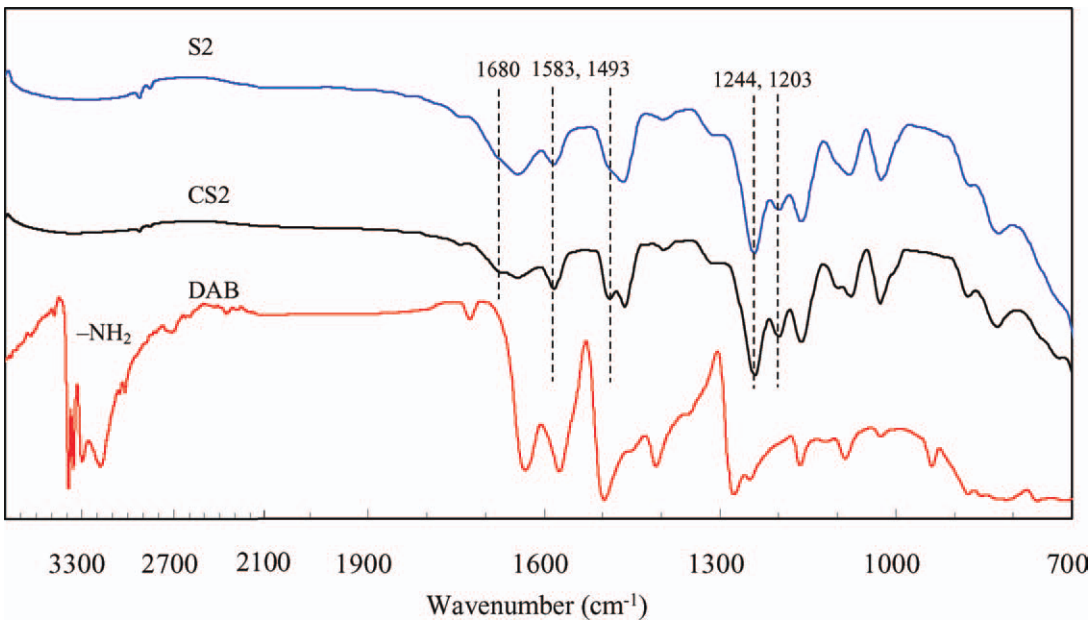

Figure 2 IR spectra of SPAES membranes and crosslinking agent DAB. [Color figure can be viewed in the online issue, which is available at wileyonlinelibrary.com]

good solubility to the polar aprotic solvents such as DMSO, NMP, and DMF, both in sodium salt and in proton form. Generally, crosslinking reduces the solubility. The crosslinked SPAESs in sodium salt form revealed reduced solubility in polar aprotic solvents, indicating the construction of the covalent crosslinking. After the proton exchange treatment, the crosslinked SPAES membranes became partially soluble only at elevated temperature in all the tested polar aprotic solvents. This suggests that the crosslinking network of the crosslinked SPAES membranes was further improved by the ionic acid-base crosslinkage between sulfonic acid groups and quinoxaline groups. However, the crosslinked SPAES membranes were partially soluble in solvents in proton form, even soluble in sodium salt form. This indicated that, for quinoxaline-based crosslinking method, the present crosslinking degree was not enough to ensure the formation of perfect network in the membranes, although crosslinking reaction was well-performed. In our previous report,[41] crosslinked SPAEKs composed of side-chain type of nonsulfonated monomer (DFB) were partially soluble in most of tested solvents in sodium salt form with QCs of 0.36–0.40 meq g^{-1}. The high solubility for present crosslinked membranes may be attributed to the introduction of flexible main-chain type of nonsulfonated monomer (DFDPS) and the slightly low QC values. To investigate the effect of QC on solubility, crosslinked SPAES membranes **CS2-2** and **CS4-2** with high QCs (above 0.50 meq g^{-1}) were prepared. **CS2-2** and **CS4-2** were partially soluble in sodium salt form and insoluble in proton form. This indicated that QC value above 0.50 meq g^{-1} was required for the formation of perfect network in quinoxaline-based crosslinked SPAES membranes. The present uncrosslinked membranes (**S1**–**S5**) containing nonsulfonated side-chain and main-chain difluoride monomers showed good solubility to the polar aprotic solvents, as similarly observed for **R2** containing nonsulfonated side-chain difluoride monomer, and also for a representative SPAES membrane **R1**, BP-SDFDPS/DFDPS(1/1). However, the corresponding crosslinked membranes revealed reduced solubility in tested polar aprotic solvents due to covalent crosslinking and the ionic acid-base interactions.

The mechanical properties of SPAES membranes are listed in Table IV, which are characterized by

TABLE III
Solubility Properties of SPAES Membranes[a]

Code	DMSO	NMP	DMAc	DMF
S1	++(++)	++(++)	++(++)	++(++)
CS1	+−(++)	+−(++)	+−(+)	+−(+)
S2	++(++)	+(++)	+(++)	+(++)
CS2	+−(++)	+−(+)	+−(+)	+−(+)
S3	++(++)	+(++)	+(++)	+(++)
CS3	+−(++)	+−(++)	+−(+)	+−(+)
S4	+(++)	+(++)	+(++)	+(++)
CS4	+−(++)	+−(++)	+−(+)	+−(+)
S5	+(++)	+(++)	+(++)	+(++)
CS5	+−(++)	+−(+)	+−(+)	+−(+)
CS2–2	−(+−)	−(+−)	−(+−)	−(+−)
CS4–2	−(+−)	−(+−)	−(+−)	−(+−)
R1	++(++)	++(++)	++(++)	++(++)
R2	++(++)	++(++)	++(++)	++(++)

[a] "++," soluble at room temperature; "+," soluble at elevated temperature; "+−," partially soluble at elevated temperature; "−," insoluble. The data in parentheses refer to sodium salt form and others refer to proton form.

TABLE IV
Mechanical Properties of SPAES Membranes[a]

Code	*M* (GPa)	*S* (MPa)	*E* (%)
S1	1.13	44	90
CS1	1.54	54	69
S2	1.07	43	59
CS2	1.26	50	33
S3	0.91	43	79
CS3	1.21	52	36
S4	0.98	48	65
CS4	1.34	61	43
S5	1.11	45	87
CS5	1.53	54	65
R1	0.89	44	42
R2	1.12	53	29

[a] *M*: Young's modulus; *S*: maximum stress; *E*: elongation at break.

Young's modulus (*M*), maximum stress (*S*), and elongation at break (*E*). All the present SPAES membranes had much higher Young's modulus and maximum stress than Nafion 112 (*M* of 0.24 GPa, *S* of 40 MPa, and *E* of 380%), and showed comparable or slightly higher maximum stress and elongation at break point than **R1** and **R2**, indicating their excellent mechanical properties. The results revealed that the incorporation of flexible main-chain difluoro monomer DFDPS was helpful to increase the mechanical properties of SPAEs. Compared to the uncrosslinked membranes (**S1–S5**), the crosslinked ones (**CS1–CS5**) showed the higher Young's modulus and maximum stress, but the smaller elongation at break. This indicates that the crosslinked SPAES membranes were slightly stiffer than the uncrosslinked ones. All the SPAES membranes were tough even in the dry state.

The thermal stability of SPAESs in proton form was examined by TGA and the results are given in Figure 3. The first weight loss observed in the range of 50–150°C was due to the loss of sorbed water. Above 150°C, the two-step degradation profile was observed for all of the membranes, as shown in Figure 3. The weight loss below 400°C was attributed to the cleavage of sulfonic acid groups, whereas the weight loss above 500°C was attributed to the decomposition of polymer backbone. The first decomposition (desulfonation) temperature (T_{ds}) was 235°C for the uncrosslinked membrane (**S1)** and 263°C for the crosslinked membrane **CS1**. The higher T_{ds} for the crosslinked membranes was caused by the acid-base interaction between sulfonic acid groups and quinoxaline groups. Although **S1** showed the slightly lower thermal stability than **R1**, the corresponding crosslinked membrane displayed the higher thermal stability than **R1** and **R2** due to the acid-base interactions.

The oxidative stability for peroxide radical attack was investigated by measuring the elapsed time that a membrane became broken after immersing the membrane sample into Fenton's reagent (3 wt % H_2O_2 + 2 ppm $FeSO_4$) at 80°C. The results are listed in Table V. The crosslinked SPAES membranes exhibited the higher oxidative stability than those of the corresponding uncrosslinked ones. This is attributed to their lower WU as well as the covalent and ionic cross-linking. Although **S1** showed the slightly lower oxidative stability than **R1**, the corresponding crosslinked membrane displayed the higher oxidative stability than **R1** and **R2**.

Water uptake, methanol uptake, solvent uptake, and dimensional change

The WU of sulfonated polymers mainly depends on the IEC,[42] and has a profound influence on the proton conductivity because sulfonic acid groups need to dissociate for protons to become mobile and transportable in membrane. So, the higher WU leads to the higher proton conductivity. However, excessive WU will result in unacceptable dimensional change or loss of dimensional shape and the dilution of the proton concentration in the membrane, which will cause a dimensional mismatch and a decrease in the proton conductivity. Therefore, a proper level of WU should be maintained in sulfonated polymer membranes in order to guarantee both the dimensional stability and the high proton conductivity.

The WU data of the uncrosslinked and crosslinked SPAES membranes at different temperatures are summarized in Table I and Figure 4. With increasing temperature from 25 to 100°C, the WU increased largely especially for the membrane with the higher IEC. It is noted that **S1** displayed slightly higher WUs than **R2** (62 and 99% at 25 and 80°C,

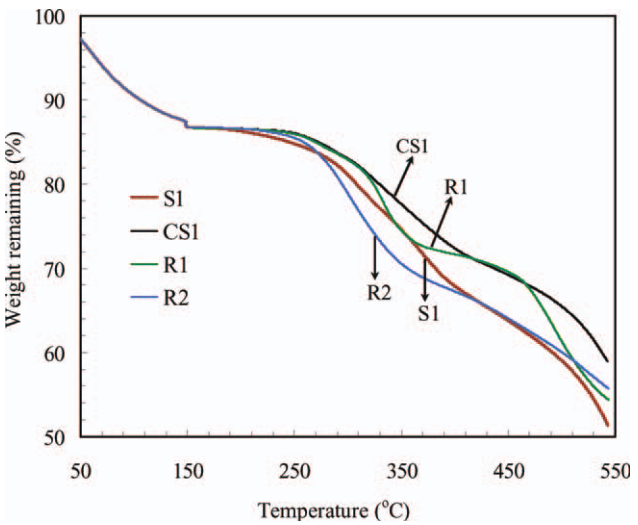

Figure 3 TGA curves of SPAES membranes. [Color figure can be viewed in the online issue, which is available at wileyonlinelibrary.com]

TABLE V
Proton Conductivity, Oxidative Stability, Methanol Permeability, and the Selectivity of SPAES Membranes

Code	σ[a] (mS cm^{-1}) 25°C	σ[a] (mS cm^{-1}) 80°C	ΔE_a (kJ mol^{-1})	τ_1[b] (min)	P_M[c] (10^{-7} cm^2 s^{-1})	φ[c] (10^4 S cm^{-3} s)
S1	96	212	11	160	10.2	9.4
CS1	62	158	15	240	5.1	12.2
S2	80	179	12	230	5.5	14.5
CS2	45	129	17	285	2.8	16.1
S3	78	192	13	250	5.4	14.4
CS3	48	147	17	330	2.9	16.6
S4	58	150	14	360	4.1	14.1
CS4	35	107	17	415	2.1	16.7
S5	60	154	14	340	4.2	14.3
CS5	38	112	17	405	2.1	18.1
R1	94	–	–	225	15.2	6.2
R2	98	197	11	125	11.6	8.4

[a] In water.
[b] τ_1: oxidative stability, refers to the elapsed time that the membranes became broken.
[c] At 32 wt % methanol solution and 25°C.

respectively) and much lower WUs than **R1** (90 and 184% at 25 and 80°C, respectively) in spite of almost the same IEC values, indicating that the nonsulfonated monomer with benzil moiety was useful to reduce the WU. Although the crosslinked membranes had the slightly lower calculated IECs than the corresponding uncrosslinked ones, the former displayed the much lower WUs than the latter, especially at elevated temperatures. For example, **CS2** showed reasonably low WUs of 30 and 54% at 25 and 80°C, respectively, whereas **S2** showed fairly high values of 48 and 105%, respectively. It is noted that the covalent and ionic crosslinking suppressed the polymer chain relaxation in water, resulting in the reduced WU. As the WU significantly depends on the IEC, the comparison of WU among membranes with different IECs is often performed in terms of the number of sorbed water molecules per sulfonic acid group (λ). The λ values were calculated using the IEC values measured by the titration method as the effective ones, and are listed in Table I. The crosslinked SPAESs showed the λ values of 11–13 at 25°C and 15–25 at 80°C, which were smaller than those (12–16 and 20–39, respectively) of the uncrosslinked ones. The λ values of the present crosslinked SPAESs with measured IEC of 1.47–1.78 meq g^{-1} were slightly higher than those (10–21) of the reported crosslinked SPAESs at 80°C with the similar IEC of 1.32–1.62 meq g^{-1},[32,40] and also slightly higher than those (12–15) of the reported crosslinked SPAEKs at 80°C with the high IEC of 1.68–2.19 meq g^{-1}.[30,31,41]

The SU and MU are also listed in Table I. As similarly observed for the WU, the crosslinked SPAES membranes displayed the much lower SUs and MUs than the uncrosslinked ones, indicating the lower methanol permeation rate when exposed to methanol solution in DMFC.

Through-plane and *in-plane* membrane dimensional changes at different temperatures were measured and the results are summarized in Table I and Figure 5. The uncrosslinked and crosslinked SPAES membranes showed the isotropic membrane swelling with $\Delta_{t/l}$ values close to unity. This is similar to the case of Nafion and SPAEs,[13,17] but different from the case of sulfonated polyimides with the larger *through-plane* dimensional change than the *in-plane* one.[10,23] The dimensional change increased with an increase in temperature and also with an increase in IEC, as similarly observed for the WU. It is noted that **S1** displayed the much lower dimensional change than **R1**, and slightly higher dimensional change than **R2**. Compared to the uncrosslinked SPAES membranes, the crosslinked ones had the

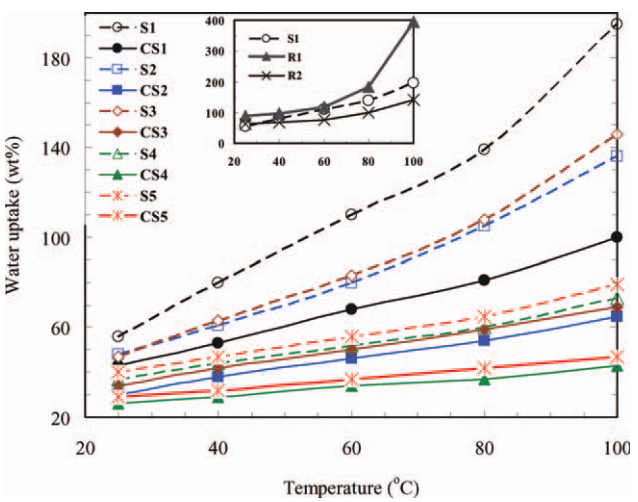

Figure 4 Temperature dependence of water uptake of SPAES membranes. [Color figure can be viewed in the online issue, which is available at wileyonlinelibrary.com]

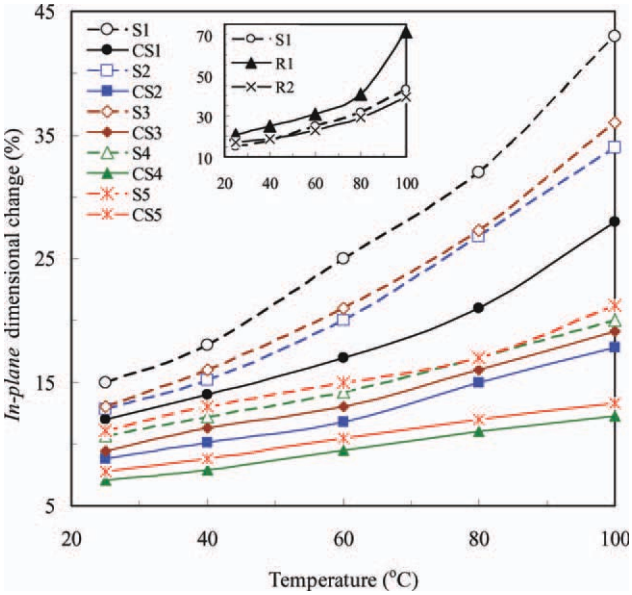

Figure 5 Temperature dependence of *in-plane* dimensional change of SPAES membranes. [Color figure can be viewed in the online issue, which is available at wileyonlinelibrary.com]

much lower dimensional change. The crosslinked membranes such as **CS4** and **CS5** showed the low *in-plane* dimensional changes less than 0.12 at 80°C, which are reasonably low for fuel cell applications.

Proton conductivity

The proton conductivity (σ) data are summarized in Table V and Figure 6. The conductivity significantly depended on IEC, WU, and temperature. The apparent activation energy (ΔE_a) of proton conductivity was evaluated in the temperature range of 25°C up to 100°C. The ΔE_a values of the crosslinked membranes were larger than those of the corresponding uncrosslinked ones. The ΔE_a values (11–17 kJ mol^{-1}) for the present SPAES membranes were comparable to those reported for SPAEs (13–25 kJ mol^{-1}).[21,22,41,43]

The SPAES membrane with the higher IEC showed the higher proton conductivity. **S1** had the highest proton conductivity of 212 mS cm^{-1} at 80°C because of the highest IEC and WU. With increasing measured IEC from 1.47 to 1.97 meq g^{-1}, the proton conductivity increased largely especially at low temperature. It is noted that **S1** displayed slightly higher proton conductivity at 25°C than **R1** in spite of the much lower WU and almost the same IEC value, indicating that the nonsulfonated monomer with benzil moiety was useful to achieve the better balance of WU and conductivity. The crosslinked membranes displayed the lower proton conductivity than the corresponding uncrosslinked ones, especially at low temperature, due to the lower measured IEC. For example, **CS5** showed low proton conductivities of 38 and 112 mS cm^{-1} at 25 and 80°C, respectively, whereas **S5** showed high values of 65 and 154 mS cm^{-1}, respectively.

The reported values of size change Δl_c and proton conductivity in water at 80°C for Nafion 117 and 1135 membranes were in the range of 0.20–0.24 and 83–125 mS cm^{-1}, respectively.[18,19,44] The corresponding values for the present crosslinked membrane (**CS5**) were 0.12 and 112 mS cm^{-1}, respectively. It is noted that **CS5** showed the much smaller size change and the comparable proton conductivity compared to Nafion membranes. On the other hand, a few crosslinked SPAES membranes have been reported to have the much larger conductivities (245 mS cm^{-1}) with the much lower WUs (23%), compared to **CS5**.[32]

Methanol permeability

The methanol permeability (P_M) and the ratio of proton conductivity to methanol permeability (selectivity, φ), which is an effective parameter to evaluate the performance of membrane in a DMFC system, are summarized in Table V. **S1** with the highest IEC (1.97 meq g^{-1}) showed the highest P_M of 10.2 × 10^{-7} cm^2 s^{-1} and the lowest φ of 9.4 × 10^4 S cm^{-3} s. For the crosslinked SPAES membranes, with decreasing measured IEC, the methanol permeability decreased much largely than the proton conductivity, and as a result the selectivity φ increased largely. **CS4** showed P_M of 2.1 × 10^{-7} cm^2 s^{-1} and φ of 16.7 × 10^4 S cm^{-3} s and **CS5** showed P_M of 2.1 × 10^{-7} cm^2 s^{-1} and the largest φ of 18.1 × 10^4 S cm^{-3} s among the present SPAES membranes. This performance was fairly high,

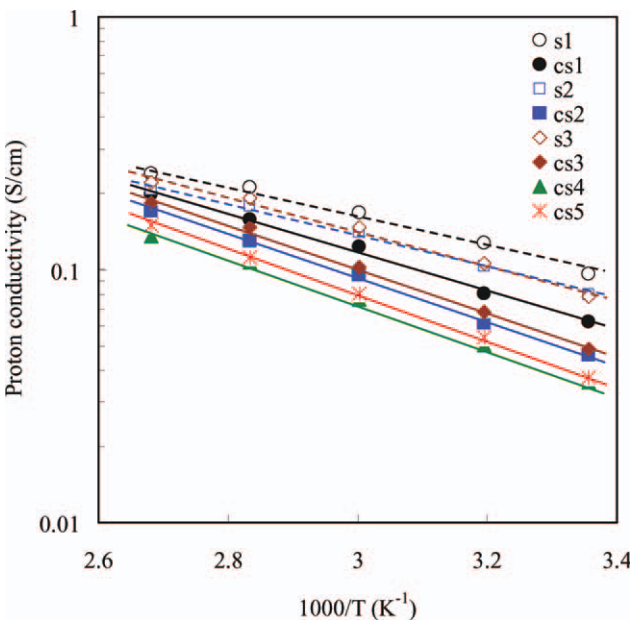

Figure 6 Temperature dependence of proton conductivity of SPAES membranes. [Color figure can be viewed in the online issue, which is available at wileyonlinelibrary.com]

taking the high feed methanol concentration (32 wt %) into account. Some comparisons are made between the present crosslinked membranes and the representative SPAEs reported in literatures[15,16,18,19,32] in terms of P_M and φ values. As the feed concentration of methanol was different from literature to literature, the rough comparison among the PEMs is preferable. The present crosslinked membranes exhibited low P_M and high φ in the range of 2.1–5.1 $\times$ 10^{-7} cm^2 s^{-1} and 12.2–18.1 $\times$ 10^4 S cm^{-3} s, respectively, which were comparable to those of the reported membranes. They have potential for DMFC application.

CONCLUSIONS

A series of crosslinked SPAES membranes were successfully synthesized by the cyclocondensation reaction of the benzil moieties in polymer chain with DAB to form quinoxaline groups acting as covalent and acid-base ionic crosslinking. The crosslinked SPAES membranes showed the high mechanical properties and the isotropic membrane swelling. They showed the lower WU, lower dimensional change, lower methanol permeability, and higher oxidative stability than the corresponding uncrosslinked membranes, with keeping the reasonably high proton conductivity. **CS5** showed a reasonably high proton conductivity of 112 mS cm^{-1}, a low WU of 42 wt % at 80°C, a low P_M of 2.1 $\times$ 10^{-7} cm^2 s^{-1} and a large φ of 18.1 $\times$ 10^4 S cm^{-3} s for 32 wt % methanol solution at 25°C, suggesting the potential application as PEMs in DMFC and PEFC. Whereas quinoxaline crosslinkages formed in the membranes sacrifice the proton conductivity to some extent due to ionic crosslinking between quinoxaline groups and sulfonic acid moieties. To improve the properties of the membranes, further investigation on the QC, nonsulfonated monomer composition, and the polymerization method is ongoing.

References

1. Kamarudin, S. K.; Achmad, F.; Daud, W. R. W. Int J Hydrogen Energy 2009, 34, 6902.
2. Liang, C.; Hisatani, H.; Maruyama, T.; Ohmukai, Y.; Sotani, T.; Matsuyama, H. J Appl Polym Sci 2010, 116, 267.
3. Mauritz, K. A.; Moore, R. B. Chem Rev 2004, 104, 4535.
4. Rikukawa, M.; Sanui, K. Prog Polym Sci 2000, 25, 1463.
5. Mehta, V.; Cooper, J. S. J Power Sources 2003, 114, 32.
6. Jones, D. J.; Roziere, J. Adv Polym Sci 2008, 215, 219.
7. Higashihara, T.; Matsumoto, K.; Ueda, M. Polymer 2009, 50, 5341.
8. Zhou, W.; Xiao, J.; Chen, Y.; Zeng, R.; Xiao, S.; He, X.; Li, F.; Song, C. J Appl Polym Sci 2010, 117, 1436.
9. Hickner, M. A.; Ghassemi, H.; Kim, Y. S.; Einsla, B. R.; McGrath, J. E. Chem Rev 2004, 104, 4587.
10. Yin, Y.; Yamada, O.; Tanaka, K.; Okamoto, K. Polym J 2006, 38, 197.
11. Chen, X.; Chen, P.; Okamoto, K. J Appl Polym Sci 2009, 112, 3560.
12. Marestin, C.; Gebel, G.; Diat, O.; Mercier, R. Adv Polym Sci 2008, 216, 185.
13. Lee, H.; Roy, A.; Lane, O.; Lee, M.; McGrath, J. E. J Polym Sci Part A: Polym Chem 2010, 48, 214.
14. Einsla, M. L.; Kim, Y. S.; Hawley, M.; Lee, H. S.; McGrath, J. E.; Liu, B.; Guiver, M. D.; Pivovar, B. S. Chem Mater 2008, 20, 5636.
15. Miyatake, K.; Chikashige, Y.; Higuchi, E.; Watanabe, M. J Am Chem Soc 2007, 129, 3879.
16. Bae, B.; Yoda, T.; Miyatake, K.; Uchida, H.; Watanabe, M. Angew Chem Int Ed Engl 2010, 49, 317.
17. Matsumoto, K.; Higashihara, T.; Ueda, M. Macromolecules 2009, 42, 1161.
18. Kim, D. S.; Robertson, G. P.; Guiver, M. D. Macromolecules 2008, 41, 2126.
19. Kim, D. S.; Robertson, G. P.; Kim, Y. S.; Guiver, M. D. Macromolecules 2009, 42, 957.
20. Hu, H.; Xiao, M.; Wang, S. J.; Meng, Y. Z. Int J Hydrogen Energy 2010, 35, 682.
21. Liu, B.; Robertson, G.; Kim, D. S.; Guiver, M. D.; Hu, W.; Jiang, Z. Macromolecules 2007, 40, 1934.
22. Li, X. F.; Zhao, C. J.; Lu, H.; Wang, Z.; Na, H. Polymer 2005, 46, 5820.
23. Bi, H.; Chen, S.; Chen, X.; Chen, K.; Endo, N.; Higa, M.; Okamoto, K.; Wang, L. Macromol Rapid Commun 2009, 30, 1852.
24. Asano, N.; Aoki, M.; Suzuki, S.; Miyatake, K.; Uchida, H.; Watanabe, M. J Am Chem Soc 2006, 128, 1762.
25. Qiu, Z.; Wu, S.; Li, Z.; Zhang, S.; Xing, W.; Liu, C. Macromolecules 2006, 39, 6425.
26. Kerres, J.; Zhang, W.; Haering, T. J New Mater Electrochem Syst 2004, 7, 299.
27. Fang, J.; Zhai, F.; Guo, X.; Xu, H.; Okamoto, K. J Mater Chem 2007, 17, 1102.
28. Mikhailenko, S. D.; Robertson, G. P.; Guiver, M. D.; Kaliaguine, S. J Membr Sci 2006, 285, 306.
29. Gu, S.; He, G.; Wu, X.; Guo, Y.; Liu, H.; Peng, L.; Xiao, G. J Membr Sci 2008, 312, 48.
30. Zhong, S.; Cui, X.; Cai, H.; Fu, T.; Zhao, C.; Na, H. J Power Sources 2007, 164, 65.
31. Ding, F. C.; Wang, S. J.; Xiao, M.; Li, X. H.; Meng, Y. Z. J Power Sources 2007, 170, 20.
32. Feng, S.; Shang, Y.; Xie, X.; Wang, Y.; Xu, J. J Membr Sci 2009, 335, 13.
33. Kerres, J.; Ullrich, A.; Haring, T.; Baldauf, M.; Gebhardt, U.; Preidel, W. J New Mater Electrochem Syst 2000, 3, 229.
34. Sen, U.; Bozkurt, A.; Ata, A. J Power Sources 2010, 195, 7720.
35. Li, H.; Zhang, G.; Ma, W.; Zhao, C.; Zhang, Y.; Han, M.; Zhu, J.; Liu, Z.; Wu, J.; Na, H. Int J Hydrogen Energy 2010, 35, 11172.
36. Lin, H. D.; Zhao, C. J.; Ma, W. J.; Li, H. T.; Na, H. Int J Hydrogen Energy 2009, 34, 9795.
37. Yang, M.; Lu, S.; Lu, J.; Jiang, S. P.; Xiang, Y. Chem Commun 2010, 46, 1434.
38. Kharlampieva, E.; Kozlovskaya, V.; Sukhishvili, S. A. Adv Mater 2009, 21, 3053.
39. Taylor, M. M. A.; Sekol, R.; Podsiadlo, P.; Ho, P.; Kotov, N.; Thompson, L. Adv Mater 2007, 19, 3859.
40. Tripathi, B. P.; Chakrabarty T.; Shahi, V. K. J Mater Chem 2010, 20, 8036.
41. Chen, X.; Chen, P.; An, Z.; Chen, K.; Okamoto, K. J Power Sources 2011, 196, 1694.
42. Fang, J.; Guo, X.; Harada, S.; Watari, T.; Tanaka, K.; Kita, H.; Okamoto, K. Macromolecules 2002, 35, 9022.
43. Zhang, Y.; Cui, Z.; Zhao, C.; Shao, K.; Li, H.; Fu, T.; Na, H.; Xing, W. J Power Sources 2009, 191, 253.
44. Pang, J.; Zhang, H.; Li, X.; Jiang, Z. Macromolecules 2007, 40, 9435.